Random Search Optimization Algorithm Based Control of Supercapacitor Integrated with Solar Photovoltaic System under Climate Conditions

I. Hamdan *‡ (iD), Amira Maghraby ** (iD), Omar Noureldeen*,*** (iD)

* Department of Electrical Engineering, Faculty of Engineering, South Valley University, Qena 83523, Egypt

** Department of Computers and Information Engineering, Thebes Academy, Qena 83523, Egypt

*** Department of Electrical Engineering Faculty of Engineering Baha University, AlAqiq 65779-7738, Saudi Arabia

(IbrahimHamdan86@eng.svu.edu.eg , Eng.amira.ieee@gmail.com , Omar_noureldeen@eng.svu.edu.eg)

‡ Corresponding Author; I. Hamdan, Qena 83523, Egypt, Tel: +201000613795,

IbrahimHamdan86@eng.svu.edu.eg

Abstract- This paper presents an optimized the control scheme of supercapacitor (SC) in grid-connected photovoltaic (PV) system by random search algorithm (RSA) under the climate conditions. The system model is consisted of 2.5 MW PV arrays generation, DC-DC converter, grid side inverter and integration with utility grid. SC is investigated with DC link of system through a bidirectional buck-boost converter circuit. The validity of SC power control unit using RSA presents a clear enhancement in system stability during variable weather conditions. The studied control design scheme is an efficient in reducing the power fluctuation under transient conditions. In addition, the optimization of SC control unit is achieved to improve its objective for damping out the oscillations and dynamic response. The RSA is categorized to optimize Proportional-Integral-Derivative (PID) SC controller to enhance its reliability during variation of climate conditions for charging and discharging modes. The simulation results were obtained for different cases such as without SC, with SC, and with optimized SC together in the conditions of various irradiations and temperatures. Also, the results showed that the optimization of SC control system could significantly improve the DC voltage stability, the active power stability, and the reactive power stability of the PV studied system. The proposed system model and the control strategy is confirmed and simulated using MATLAB/SIMULINK environment. Furthermore, the validity of the proposed technique is described by comparing the results.

Keywords- Photovoltaic System (PVS), Supercapacitor (SC), Proportional-Integral-Derivative (PID) controller, Power Control, Random Search Algorithm (RSA) optimization.

1. Introduction

The growth of energy demand and conservation of natural environment is important due to the unreliability of fossil fuels. The renewable energies play a vital role for ensuring the long-term viability of grid systems [1]. Solar and wind energy, for example, are not only sustainable, but they also aid to prevent environment pollution [2]. Furthermore, the relatively low cost of required components for green sources means that more applications in this sector can be located across the world [3]. Photovoltaic systems (PVSs) have a lot of benefits over wind systems (WS), including the elimination of mechanical parts, maintenance free, and easy installation [4]. Solar energy optimization is constantly being updated, which contributes in recognizing its effectiveness in many fields [5, 6]. Moreover, among the most significant challenges that PVS applications are encountered is the climate condition. As a result, research strategies in PVS applications should take it into consideration. The generated

energy of PV arrays is regulated by environmental factors as temperature and irradiation, the results in a rapid shift in energy conversion efficiency [7, 8]. As a result, this mission might be accomplished with need for maximum power point tracking (MPPT) when using a control unit on the DC link to manage the DC voltage and absorb peak power of PV arrays even in bad conditions [9, 10]. Significantly, output characteristic of a PV cell varies with weather factors as temperature and irradiation and also they control the generated amount of energy [11]. Variable radiation and temperature are the main issues through it PV arrays cannot generate the full efficiency to generate the main power for system [12]. As a result, it is needed to use a backup power source to optimize any fluctuations occurs in generated power during these conditions [13]. Nowadays, Energy Storage Device (ESD) is the most important technology has been applied in the renewable systems during random variations. The most common ESDs have been used in PVSs are battery and supercapacitor (SC). SCs have a lot of

benefits over normal types of capacitors or batteries [14]. It has a high density of storage power, low charge and discharge period, long lifecycle and leakage current is very low as well as its internal resistance. Also, SCs are used as physical backup power supplies because they have super storage capacity of energy. The energy flows in and out of SC model elements also, it changes depending on the instantaneous generated and grid conditions [15]. On other side, during fast transient condition, batteries could not deliver energy to the system also, it has high cost and low life long [16]. A lot of researches have studied the stability of PVS at variable conditions using ESD. In [17] minimize the fluctuation of power in grid-connected PVS using SC during increasing and decreasing irradiation is studied. In [18] the operation of PVSs during change in climate condition with a hybrid ESDs (battery and SC) is demonstrated. In [19, 20] an approach technique that has used SCs to reduce power fluctuations in PVS at the point of common coupling (PCC) under irradiation condition is presented. In [21] improvement power quality under the disturbance of systems using ESD, which reduces the power fluctuations have been presented. Buck-boost converter circuit is implemented in SC model to control charge and discharge [22]. There are two modes of operating system for converter circuit, during a charge mode is a buck and in discharge mode is a boost [23]. Power control unit is used in converter circuit to regulate power fluctuation of system during variations in climate conditions [24]. Effect of high irradiation on grid-connected PV system has been investigated in [25-28]. In [29] tests a random of solar irradiance with continuous variations load, system is examined under variable irradiance conditions. In [30] a 300W standalone PV system analyses the charging time of battery and SC with variable irradiation. Proportional-Integral-Derivative (PID) controller is used in engineering application to enhance steady-state or transient behaviours. PID is commonly used as it has many advantages as less maintenance and simple structure cost [31]. A lot of PID optimization techniques have been used such as genetic bayesian optimization (GBO), dynamic programming (DP), particle swarm optimization (PSO), game theory (GT), sequential optimization (SO), gradient descent (GD), greedy control (GC), genetic algorithm (GA) and random search algorithm (RSA) [32]. RSA is the most popular method as has a wide range of applications to solve the complex problems. This algorithm method has some advantages as its implementation is so easy with the complex problems and it has a potential to get the solution of the large-scale problems efficiently. RSA is applied to design the self-tuning of PID controller to optimize the work of controller. A lot of researches have studied the potential improvement to adjust PID parameters to modify its performance with power systems applications [33]. RSA methodology focuses on presenting an integrated optimized PID controller for renewable system [34]. Potential improvement of control unit optimization to modify ESD charging and discharging with system applications has been studied in [35]. In [36] RSA performance with MPPT for tracking the peak power during variety of irradiation compared with two-stage perturb and observe (P&O) and particle swarm optimization (PSO) method is studied. Considering all the issues summarized above, this paper is focused on improving the dynamic

capability of a grid-connected 2.5 MW PVS with SC during variation of climatic conditions. For this purpose, the optimal SC control method is designed for decreasing the PV power fluctuations caused under changing in irradiation and temperature. The studied optimization algorithm namely the RSA is used to tune the SC control parameters. Moreover, the PID controller using RSA technique has been used for buck-boost converter to control operation modes of fast charging and discharging rate of SC. On the other hand, an optimized PID control scheme for SC integrated with solar PVS is designed to regulate DC link voltage and improve the active and reactive power of the system. Many scenarios with a comparison study are tested for temperature and irradiation conditions to check the efficiency of the proposed technique. The contents of this paper are presented as follows: Section 2 modelling and control of PVS. Section 3 illustrates model and control of SC. Section 4 focuses on optimized technique of RSA. Section 5 illustrates the studied system with SC connection. Section 6 presents the simulation results.

2. Modelling and Control of PVS

Solar panel contents several numbers of PV solar cells. Depending on the type of material used, a single tiny cell could also provide between 1 and 2 W of power. PV cells are made up of a semiconductor or material with P-N junction. It can be joined together to produce a high module for increasing the output efficiency. The highest power capacity of the module is 1 kW; even if larger capacities are feasible to make, handling more than 1 kW modules will really be difficult. A collection of modules can be interconnected to form an array dependent on the capacity of the power plant or the amount of power supplied [37]. Figure 1 illustrates the equivalent circuit of single solar cell component. The semiconductor material is the main components in cells of PV panels. This semiconducting material transfers the photons of sun light to electrical energy, so this layer works as a current source. The generated DC current passes through some internal components of the cell as a single diode with a shunt resistance and they are connected to a series resistance [1, 4]. The total current of PV model is elaborated as follows.

$$I_{PV} = I_{ph} - I_D - I_{pa} \tag{1}$$

where I_{PV} is the output current of the PV module, I_{ph} is the generated photocurrent of the cell, I_D is the diode current and I_{pa} is the leakage current through the parallel resistance (R_{pa}). I_D current which depicts the recombination losses in the PV module is expressed as follows.

$$I_D = I_0 \left(\exp\left(\frac{V_D}{V_{th}}\right) - 1 \right) \tag{2}$$

where I_0 is diode saturation current, V_D is the diode voltage, V_{th} is thermal voltage of PV module cells and it is illustrated as follows.

$$V_{th} = \frac{AKTN_s}{q} \tag{3}$$

where T is cell temperature, A is the diode ideal factor (1<A<1.5), q is electron charge of (p-n) junction = (1.602 ×

10-19 C), N_s is the series number of cells and K is Boltzmann constant = (1.3806 ×10-23 J/K).
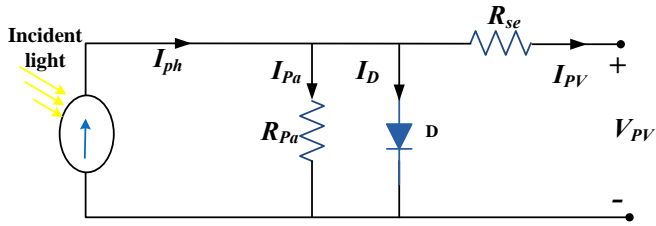

Fig. 1. Equivalent circuit of a single solar cell.

Voltage diode and current across parallel resistance can be calculated based on a simple Kirchhoff's current law (KCL) as follows.

$$V_D = V_{PV} + I_{PV} R_{se} \tag{4}$$

$$I_{Pa} = \frac{V_{PV} + I_{PV} R_{se}}{R_{pa}} \tag{5}$$

where V_{PV} is output voltage of PV and (R_{se}) is the module series resistance [18, 38].

Figure 2 shows a DC/DC converter circuit with MPPT unit. The DC/DC converter is used to connect the DC side with the generated unit. It is consists of a filter capacitor (C_f), diode (D) and an inductor (L_f) with IGBT switch. Also, it differs according to its levels of complexity, as most of them used digital processors and others can be implemented using analogy components. The MPPT unit is used to regulate the optimum value of DC voltage and power to set the maximum generated values. The P&O technique is a popular MPPT technique since it just requires PV voltage, current and is therefore simple to implement [39-41].

Grid inverter control unit is designed to implement the generated power of grid-connected PV system. This unit consists of double control loop. They are composed by a current loop and an outer voltage loop [42]. The methodology of grid inverter control unit is investigated by coupling both the current control as an inner loop and voltage control as an outer loop. The inner control unit is simplified by taking the reference active current Id that is generated from outer loop. But, the reactive current (I_q) sets at zero to stabilize unity power factor because at normal operation the reactive power of grid side inverter has a zero value [43, 44].
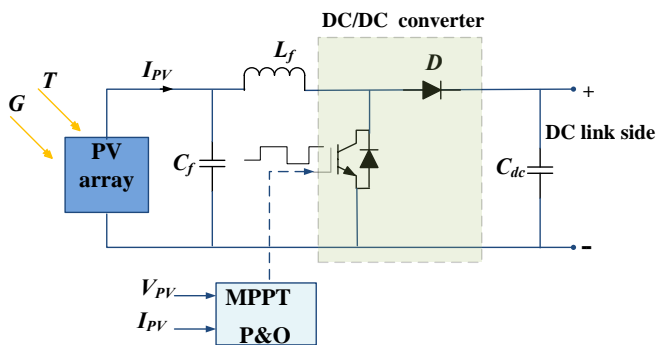
The control strategy of outer loop is related to DC link voltage. DC voltage (V_{dc}) is stabilized at normal using the voltage control unit. The active current reference is the output of outer loop. The schematic diagram of control strategy for grid side inverter is shown in Figure 3.

The following equations show the mathematical description of grid side inverter voltage in d-q axis control unit.

$$I_{dref} = K_P \left(V_{dcref} - V_{dc} \right) + K_I \int \left(V_{dcref} - V_{dc} \right) dt \tag{6}$$

$$V_q = K_{P_1} \left(I_{qref} - I_q \right) + K_{I_1} \int \left(I_{qref} - I_q \right) dt \tag{7}$$

$$V_d = K_{P_2} \left(I_{dref} - I_d \right) + K_{I_2} \int \left(I_{dref} - I_d \right) dt \tag{8}$$

where I_{dref} is the reference d axis component of grid current, V_{dcref} is the reference value of DC voltage, K_P and K_I are PI gains of DC controller. V_q is q axis component of inverter voltage, I_{qref} is the reference q axis component of grid current, I_q is q axis components of inverter current, K_{P1} and K_{I1} are gains of first current controller. V_d is d axis component of inverter voltage, I_d is d axis components of inverter current, K_{P2} and K_{I2} are gains of second current controller. The active and reactive power of grid side P_g and Q_g can be illustrated as follows with the d-q voltages (V_{gd}), (V_{gq}) and the d-q currents (I_{gd}) and (I_{gq}) [45, 46].

$$P_g = \frac{3}{2} \left(V_{gd} I_d + V_{gq} I_q \right) \tag{9}$$

$$Q_g = \frac{3}{2} \left(V_{gd} I_d - V_{gq} I_q \right) \tag{10}$$

Fig.2. DC/DC Boost converter circuit with MPPT unit.
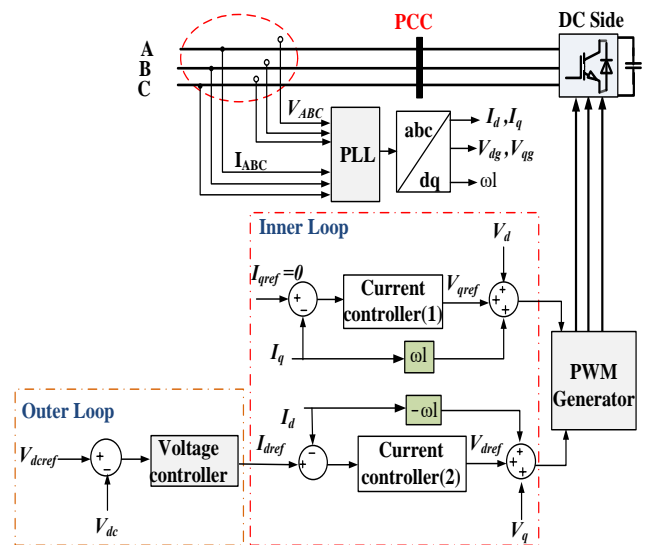

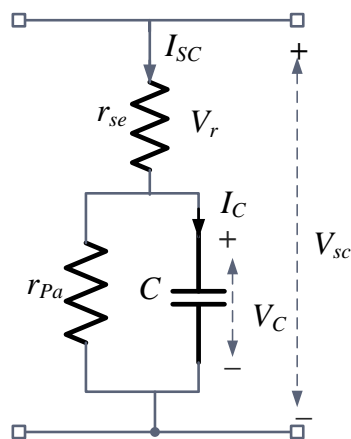**Fig. 3.** Schematic diagram of control strategy for grid side inverter.

Fig. 4. Equivalent circuit of SC model.

3. Modelling and Control of SC

SCs are electrochemical devices that are classified as ESDs. It offers many benefits that keep it a popular option in renewable systems. It has a high power density, a long lifetime, low inner impedance, and it is almost efficient. They may be utilized to control the rapid volatility in power generation of renewable energy systems [47]. It is used to stabilize the power of DC side according to the MPP strategy during excessive power fluctuation. In comparison with batteries and ordinary capacitors, SC is a low-maintenance device that can be used for a variety of energy-system applications [48]. Table 1, shows the comparison between the characteristics of three types of ESDs as SC, batteries and normal capacitor. The main electrical diagram of SC model is shown in Figure 4. It consists of a parallel resistance r_{pa} with main capacitor C and they are connected to a series resistance r_{se}. The series resistance is used to reduce the internal heating of capacitor during the charge and discharge modes. On the other hand, the parallel one is used to reduce the leakage current, also increase the time of storage energy [49]. The methodology of SC capacity depends on energy management strategy. SC generally has low energy and high peak power, so it works as an auxiliary power source that should inject power back during the transient modes. SC has properties of fast charge/discharge and it provides a high power to system in a short time during a fast transient. SC also achieves the balance in power flow at DC bus through buck/boost converter duty cycle as it varies between 5 % and 80% to keep DC bus voltage and current stables [20, 37, 50]. The model of SC can be illustrated as follows.

$$Q = C\, V_C \tag{11}$$

$$\frac{dQ}{dt} = I_C(t) \tag{12}$$

$$\frac{dV_C}{dt} = \frac{1}{C} I_C \tag{13}$$

$$V_r(t) = r_{se} I_{SC}(t) \tag{14}$$

$$V_{SC}(t) = V_C(t) + V_r(t) \tag{15}$$

Table 1. Characteristics of different types of ESDs.

Characteristics	Batteries	Capacitors	SC
Life cycle	$\sim= 1000$	∞	$\geq 5e^6$
Charge / Discharge time	1 – 5 h 0.03 - 3 h	$10^{-6} - 10^{-3}$	Sec or min
Efficiency (%)	85	95	99
Rated power(W/kg)	≤ 1000	≥ 10000	≤ 19.6
Rated energy (Wh/kg)	≤ 1606	< 0.1	≤ 1091

where Q is capacitor charge, C is capacity of capacitor, V_C is voltage across C, I_C is current through C. V_r is voltage across r_{se}, V_{SC} is voltage of SC and t is charging and discharging time. The following equation illustrates the capacity size of capacitor in SC model in Farad.

$$C = \frac{\int_{t_0}^{t_1} I_C(t)\, dt}{(V_{C1} - V_{C0})} \tag{16}$$

where V_{C0}, V_{C1} are minimum and maximum voltages across C, t_0 and t_1 are minimum and maximum voltages times.

Performance of SC depends on MPP methodology of PV generated power. If any transient occurs, the generated PV voltage is fluctuated, and then power is fluctuated. But, SC can storage an extra power during the variable conditions and recharges it to recover this disturbance that has been occurred [51]. In Figure 5, the control circuit of SC is shown. It consists of SC model with a connection of a bidirectional buck/boost converter circuit. The converter circuit consists of two IGBTs switches M1, M2 and an inductor (L). The storage energy of SC E_{SC} is desorbed as follows.

$$E_{SC} = \frac{C\, V_C^2}{2} \tag{17}$$

P_{SC} is SC power in watt with relation to grid power P_g and PV generated power P_{PV} can be illustrated as follows.

$$P_g = P_{PV} \pm P_{SC} \tag{18}$$

The buck mode of the bidirectional circuit is the charging mode, in which current injects via SC. Furthermore, the discharging mode will be when the DC current flows out of the SC, and the operation of bidirectional circuit is as a boost

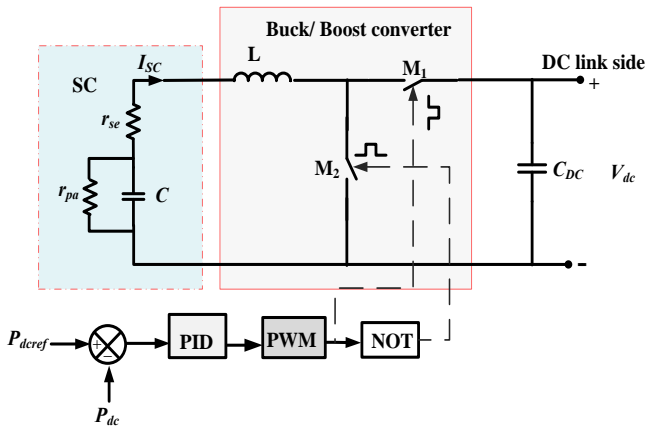mode. The voltage and current through SC are depicted as follows.

Fig. 5. Configuration of SC control circuit.

$$V_{SC} = I_{SC}\, r_{se} + \frac{1}{C}\int\left(I_{SC} - \frac{V_C}{r_{pa}}\right) dt + V_{C.0} \qquad (19)$$

where I_{SC} is SC current and $V_{C.0}$ is initial voltage on SC.

Bidirectional buck-boost converter circuit is usually used to control SC operation modes of charging and discharging. SC can be used to stabilize output power of system at a constant value. Regulation output power that between the DC side and SC is through a power control unit for SC model. A buck-boost converter with the power control unit and a SC model are shown in Figure 5. In this control technique, DC power (P_{dc}) is measured and compared with the reference value (P_{dcref}). The output signal drives the controller of PID then the signal output is compared with pules width modulation (PWM) to generate duty cycle [52]. The main control pulses for switches, which need for a NOT gate to inverse from each other is presented as follows.

$$D_{ut} = (K_p + \frac{K_i}{s} + K_d s)\,(P_{dcref} - P_{dc}) \qquad (20)$$

where D_{ut} is the output duty cycle, K_p, K_i and K_d are the parameters of PID controller.

4. PID Control Based on RSA Optimization

RSA uses random numbers which can be used for minimization and maximization methods. This algorithm works by moving and generating random solution vector in next iteration from the best solution achieved so far towards an optimal solution [53]. Additionally, the RSA is chosen because of its ease of implementation and requirement of less adjusting parameters. RSA algorithm is used to optimally design the PID power controller of SC. PID controller has been generally used in standard control of processes and systems. The main objective of PID controller is to adjust input signals to be as same as the feedback signals during any external disturbance [54, 55]. An optimal control technique with use of RSA optimization, is implemented as a control strategy for tuning the controller of SC for the integration of the studied PV system into the grid. Therefore, the objective function is considered the sum of the integral squared errors of PID controller as follows.

$$ISE = \int_0^\infty e^2(t)\, dt \qquad (21)$$

where ISE is the integral square error and $e(t)$ is error between the output and input signals of controller.

In Figure 6 shows the general flow chart and the steps that describe the operation of RSA method [53] as follows.

1. Initialize the solution vector randomly y_i between [y_{min}, y_{max}], set maximum number of iterations k, initial step length l, and number of variables in the optimization method N.

$$y_i = [y_1, y_2, y_3, ..., y_N]$$

2. Evaluate the objective function value f(y_i).

3. Generate a set of N random numbers as follows:

$$u = [r_1, r_2, r_3, ..., r_N]$$

4. Calculate the new selecting solution vector as follows:

$$y_i = y + lu$$

5. Evaluate the corresponded objective function value $f(y)$ and then compare with the previous function value $f(y_i)$.

6. Select new value as follows

$$if\ \ f(y) < f(y_i)\ then,\ y = y_i\ \ and\ f(y) = f(y_i)$$

7. Test the termination criteria, if it is satisfied, go to step 9 else, go to the step 8

8. Calculate the new reduced in step length to get adaptive step algorithm size $l = l\ C$ and return to step 4.

9. Stop the RSA and take $y_{opt} = y_i$ and $f_{opt} = f(y_i)$

The RSA parameters that used in this paper are as follows: numbers of iterations are $N =100$. RSA coding selects the variable numbers of PID parameters as K_p, $K_i \in [0, 1500]$, and $K_d \in [0, 2]$. Fitness function is implemented using MATLAB/Simulink, during PVS is run in time t. The optimal value is calculated in Simulink before sending to the MATLAB workspace according follow equation.

$$ISE(y_1, y_2, y_3) = \int_0^t (P_{ref} - P_{dc})^2(t)\, dt \qquad (22)$$

where y_1, y_2 and y_3 are K_p, K_i and K_d

The connection of SC PID controller with studied system using RSA technique as shown in Figure 7. At last, the optimized of PID parameters is inserted to Simulink at the time of the maximum iterations is reached. Finally, the optimal parameters obtained are:

$K_P= 1.2027e^3$, $K_i= 955.2554$ and $K_d=0.9825$.
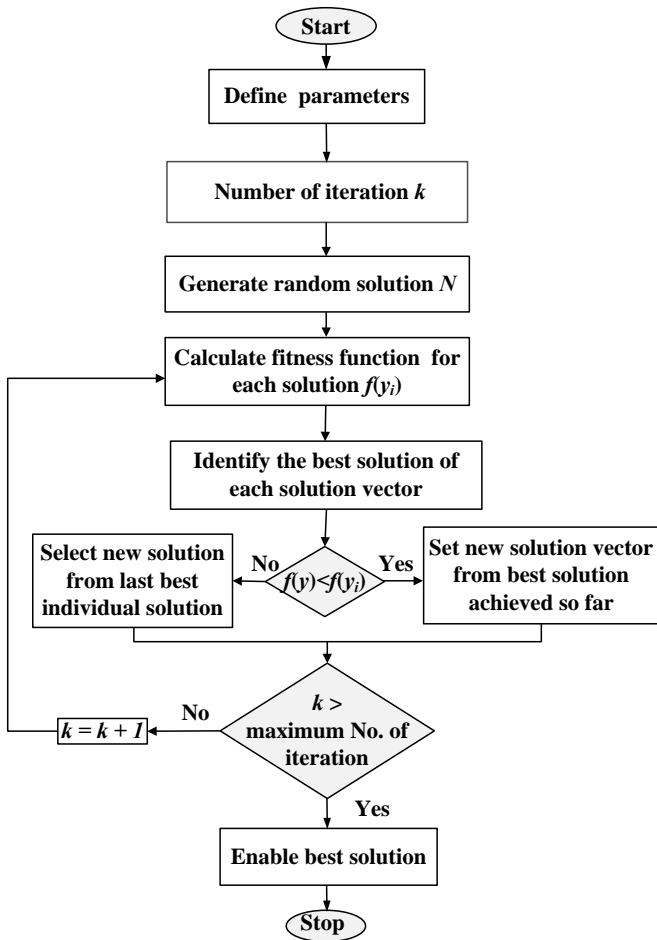
Fig. 6. Flowchart of RSA method.

5.   Establishment of Studied System

The establishment of the studied system is depicted as shown in Figure 8. Solar panels or PV arrays, MPPT control unit, DC/DC converter, DC/AC inverting unit, three phase transformer, and utility grid are the main components of a PVS. The sunlight is transformed to electrical energy through the PV arrays, and the MPPT controller subsequently stabilizes the generated power and voltage to the maximum value for optimal advantages. The DC voltage is converted to a regulated voltage via DC/DC converter. After that, a DC/AC inverter converts the DC power from the PV arrays into AC voltage, which is then fed into a step up transformer to provide the utility grid or a fixed load. The PV arrays in the case study model are organized into ten rows of PV modules linked in parallel. Each row generates a certain active power 250 kW, and the rated active power of groups is 2.5 MW. Providing a fixed output DC voltage, a step-up boost DC/DC converter is required to generate rated voltage 700 V. In most applications, the MPPT is connected to the DC/DC converter to adjust the duty cycle. The sort of MPPT employed in this system is a P&O type. A parallel connection of SC model with DC link capacitor and a major power control unit of bidirectional buck/boost converter circuit are provided through each row of PV arrays to dc filter capacitor. DC/AC inverter with a filter unit transfers the power and voltage to utility grid through a transmission line with three phase step-up transformers. The specifications of PVS that is used in this study are described **Table. 2**
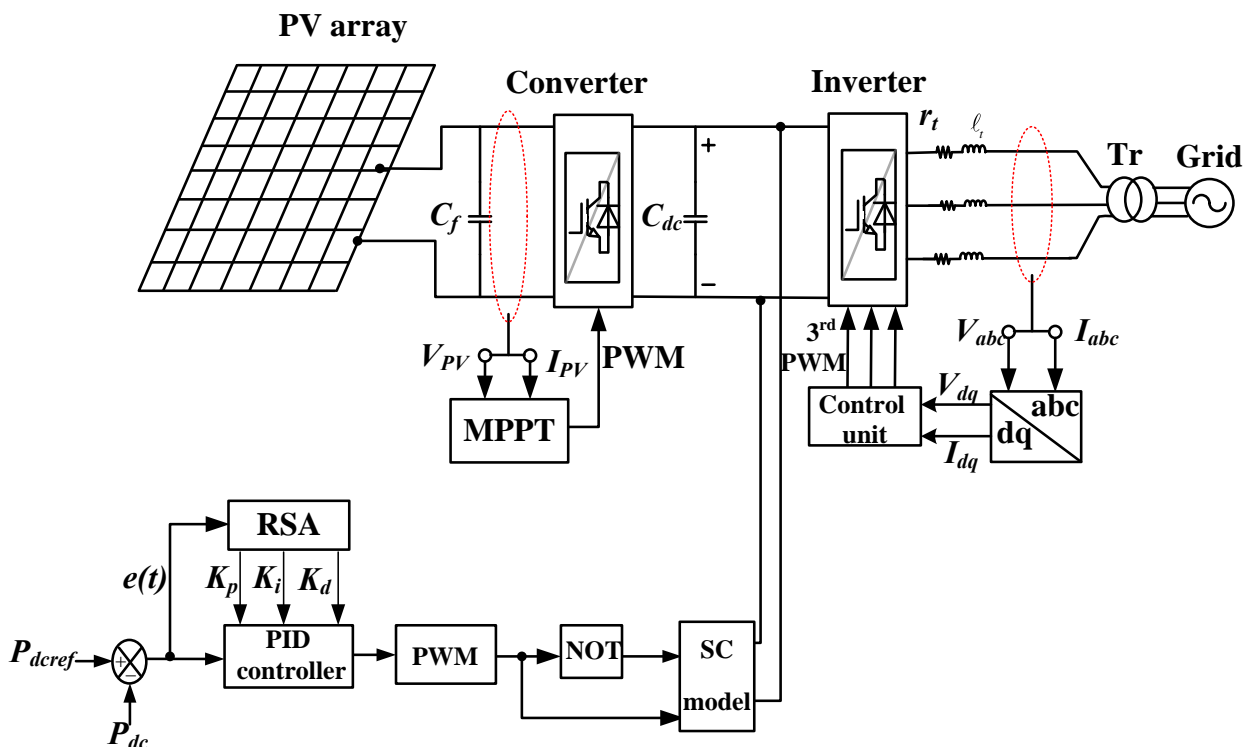

Fig. 7. Grid-connected PV system with RSA method.

Table 2. Simulation parameters of studied system.

Parameter	Value
PV parameters	
Rated power (P_{PV})	2.5 MW
Rated voltage (V_{PV})	700 V
DC link capacitor (C_{dc})	50 e^{-3} F
Boost converter parameters	
Inductance (L_f)	5e^{-3} H
Resistance (R_f)	5e^{-3} Ω
Filter capacitor (C_f)	100e^{-6} F
SC model parameters	
SC capacitance (C)	400 F
Inductance (L)	9.9e^{-3} H
Inverter parameters	
Filter resistance (r_t)	1e^{-3} Ω
Filter inductance (ℓ_t)	45e^{-6} H
Grid parameters	
Rated voltage (V_g)	220 kV
Rated frequency (f)	50 Hz

6. Simulation Results

The efficiency of the proposed RSA algorithm for SC equipped with grid-connected PV system during different climate conditions of irradiation and temperature is analysed, where the DC voltage, active power, and reactive power is monitored. In order to test the performance of studied methodology of grid-connected PV system in cases of without SC, with SC, and with optimized SC, the study is simulated in MATLAB/Simulink software. The system is tested under following cases; Normal condition is presented for a standard radiation and temperature (1000 W/m^2 and 25 ºC). Variable irradiation (1000 – 1500 – 800 – 1000) W/m^2 with constant temperature at 25 ºC is analysed. Random irradiation condition over a day is also tested. During constant irradiation at 1000 W/m^2 and variable temperature around (20 – 25 – 35 – 45) ºC is examined. Each case is performed on grid-connected PV system to analysis its parameters performance.

6.1. Normal Operation of Studied System

Power system generates the rated values of 700 V of DC voltages, 2.5 MW of active power and zero of reactive power under standard conditions, which are generally delivered to the grid. Figure 9 shows the DC voltage, active power, and reactive power of system characteristics. The correction of losses only results in 20 kW difference between both the generated and grid sides. Figure 9(a) shows the maximum produced PV voltage (V_{PV}) with reference value (V_{ref}) 700 V. Using MPPT and the converter circuit, (V_{dc}) is also kept constant with the reference value. In Figure 9(b), the control unit of grid side inverter delivers 2.5 MW to the grid as the maximum power (P_{PV}). Also, shows the absorbed power on SC is zero at normal operation of system. In Figure 9(c) shows the reactive power at normal value 0 VAR.
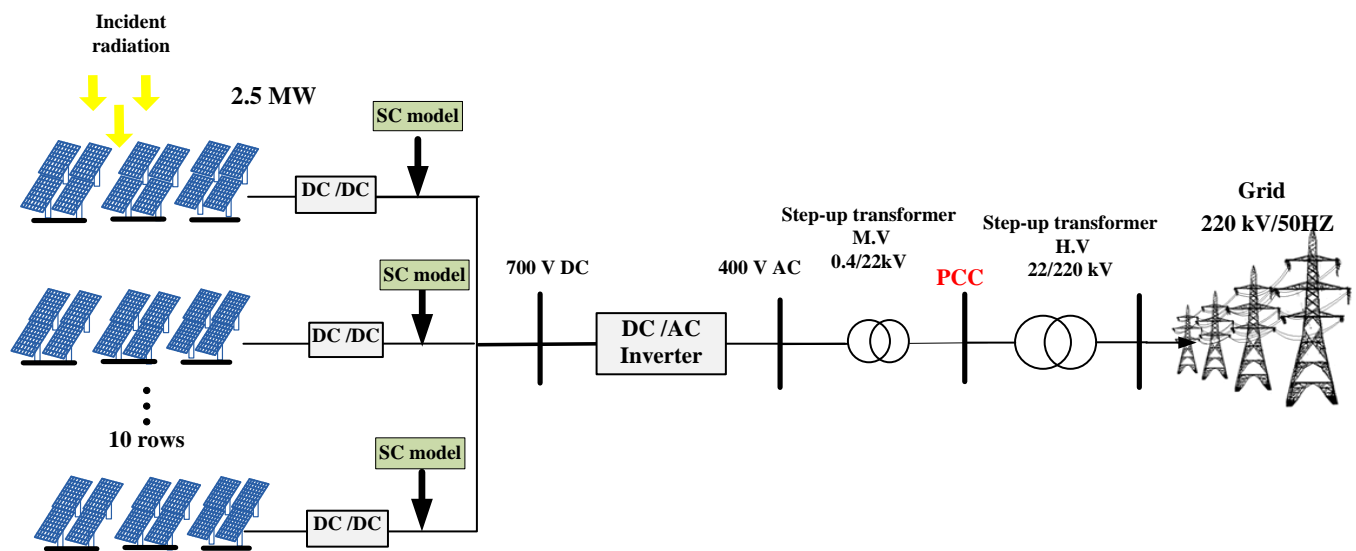

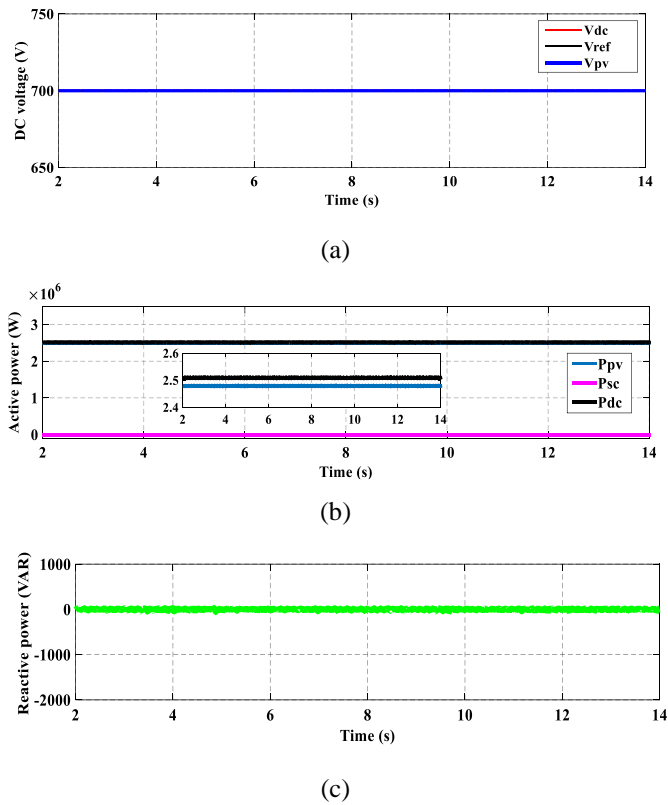**Fig. 8.** Studied 2.5 MW PV system diagram.

(a)

(b)

(c)

Fig. 9. System performance during normal condition. (a) Output voltages. (b) Active powers. (c) Reactive power.

6.2. Variable Irradiation Conditions

In Figure 10(a), irradiation varies between 1000 W/m^2 to 1500 W/m^2 during interval from 11 s to 11.25 s then decreases to 800 W/m^2 for 11.5 s after that, it is normally stabilized at 1000 W/m^2. As shown in Figure 10(b) DC voltage in case of without SC is increased to 750 V during then decreasing to 610 V. With SC power control using RSA type, the DC voltage is stabilized at normal value 700 V. When using trial and error method, the voltage has small oscillations around rated value. In Figure 10(c) shows the active power performance during change of irradiation. Without SC, it is increased to 3.5MW then, decreased to 0.5 MW. With SC, using RAS, it increases to only a small value to 2.55 MW. Also, when radiation decreases, the active power is decreases to 2.48 MW. With trial and error, active power is stabilized at rated during irradiation increased, but during irradiation reduction, it decreases to small value 2 MW. In Figure 10(d) shows a high reflection in reactive power in case of without applied SC. The reactive power increases to 1 MVAR. Also, during the reduction of radiation, it decreases to -1 MVAR. On the other side, with SC, the results of reactive power for both RSA method show less oscillations than thus occur when using trial and error method.
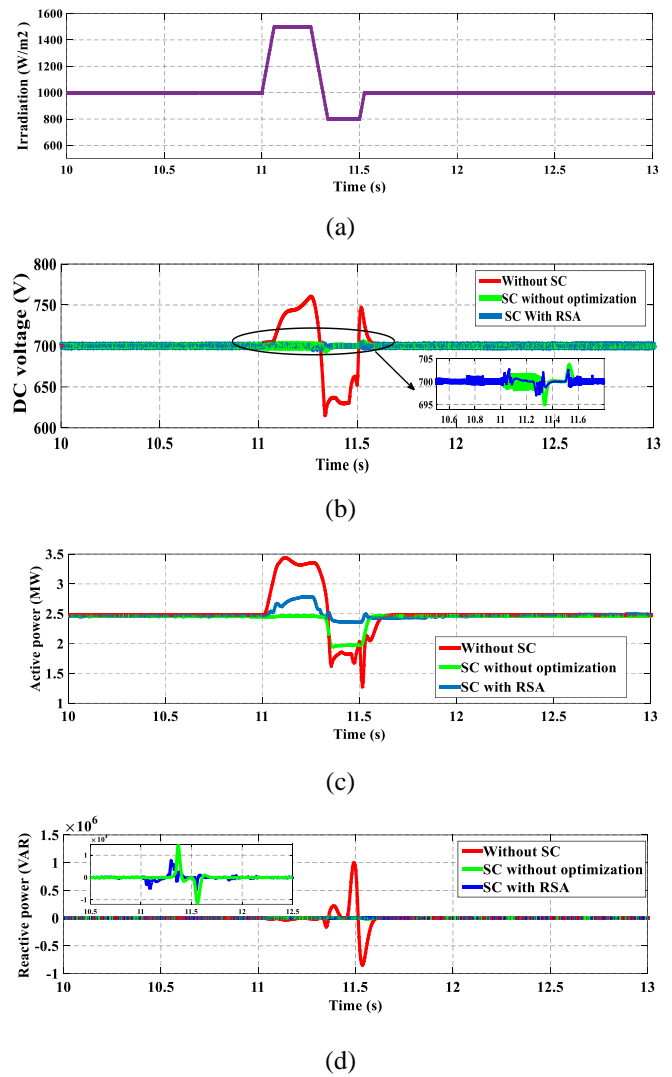

(a)

(b)

(c)

(d)

Fig. 10. System performance during variable irradiation conditions with different schemes. (a) Variation of irradiation condition. (b) Output DC voltage (c). Active power (d) Reactive power.

6.3. Random Irradiation Condition

In Figure 11(a), shows a random radiation for a daily sun shine. As shown in Figure 11(b), the DC voltage has a high oscillations without SC, it increases from 745 V to 640 V also from 750 V decreases to 625 V then increases to 800 V. On the other hand, with SC using RSA, the DC voltage is stabilized at normal value 700 V. With trial and error method, it has some oscillations as the case of without SC. In Figure 11(c), shows the active power without and with SC. Without SC, active power has high fluctuations, but fluctuations are not so high with SC connection using RSA. Also, these fluctuations are the same when using trial and error type as without SC.

In Figure 11(d), the reactive power is oscillated from 0.25 MVAR to -0.25 MVAR then fluctuates again from 1 MVAR to -1 MVAR. With SC and RSA, the reactive power is stabilized at zero. During using trial and error type, the reactive power has same performance as without SC.

6.4. Variation of Temperature Condition.

In Figure 12(a), shows the applied temperature between minimum 20 ºC to maximum 45 ºC at constant radiation of 1000 W/m². As shown in Figure 12(b), the DC voltage has decreased to small value in case of without SC, but with SC using RSA, the DC voltage has nearly low oscillated over rated value. In Figure 12(c), shows the active power, without SC, it has oscillated with change of temperature, but fluctuations are null with SC. In Figure 12(d), the reactive power is high oscillated without SC if compared the case of with SC connection. During using trial and error type, the DC voltage, active power and reactive power reactive power have high oscillations than with RSA.
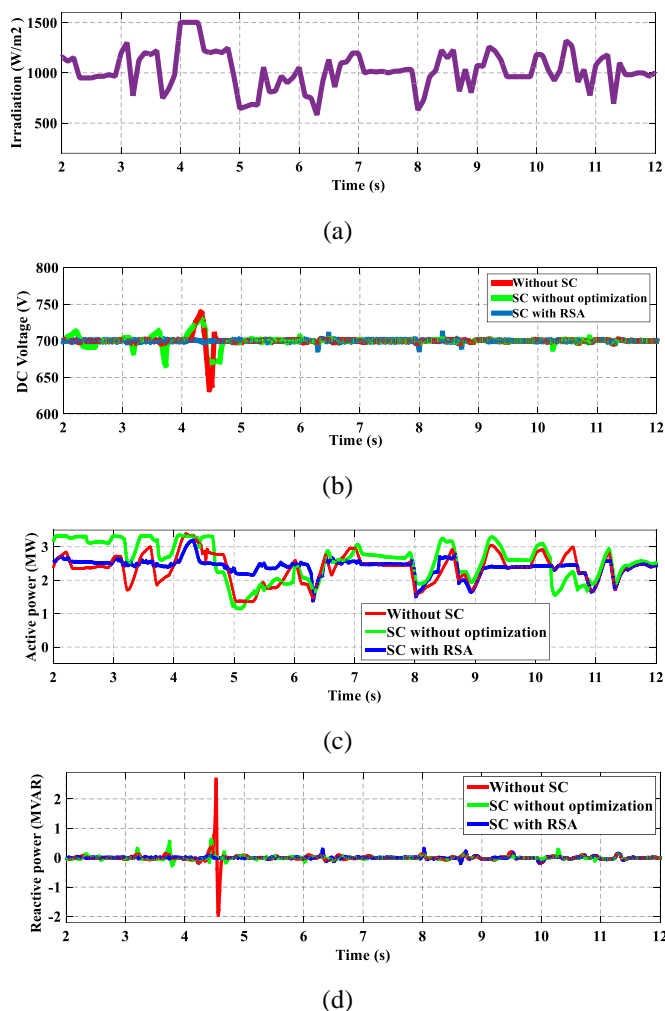

(a)

(b)

(c)

(d)

Fig. 11. System performance during random conditions with different schemes. (a) Applied random radiation. (b) DC voltage. (c) Active power. (d) Reactive power.
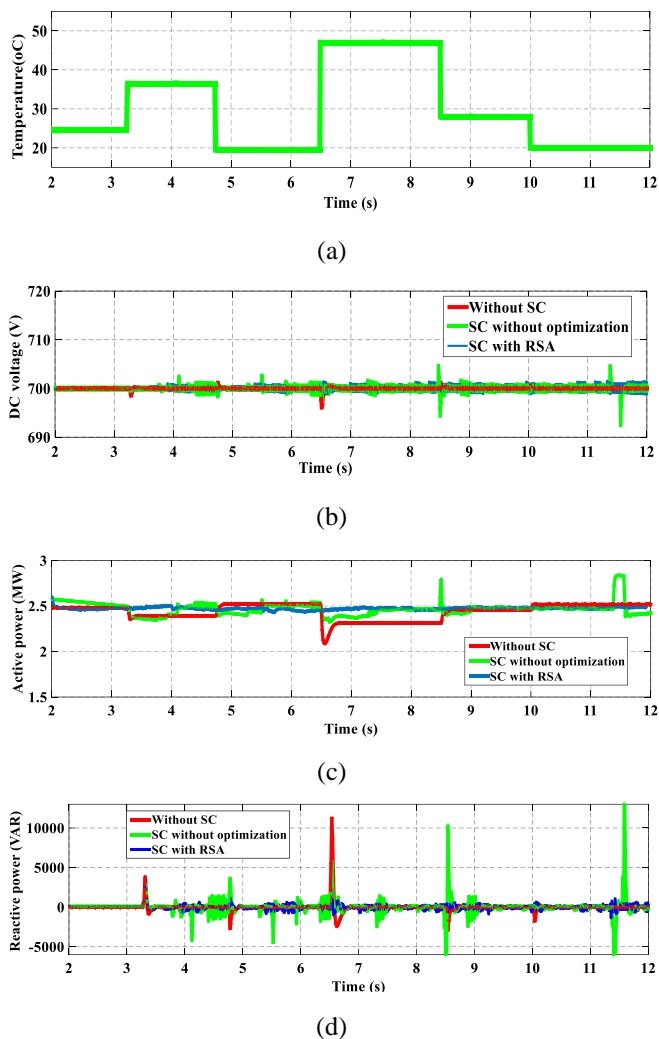

(a)

(b)

(c)

(d)

Fig. 12. System performance during variable temperature conditions with different schemes. (a) Variation of temperature condition. (b) DC voltage. (c) Active power. (d) Reactive power.

7.   Conclusions

This paper mainly focuses on the reduction of power fluctuation for grid-connected 2.5 MW PVS using SC. SC is an ESD and is implemented as a solution for the system disturbance. SC banks are connected in parallel to DC link side using a buck-boost converter for charging or discharging the extra power. Optimized PID parameters approach using RSA enhances the SC control unit efficiency. The design and analysis of the proposed control scheme investigates to improve the dynamic response, stability, and power quality of the studied system under the climate conditions. The validity of system parameters such as DC voltage, active power, and reactive power have been investigated in cases of without SC, with SC and with SC optimization. During irradiation variation and constant temperature, the DC voltage, active power and reactive power are fluctuated very high when the system operates without SC.

With SC using RSA optimized technique for control unit, the system parameters are stabilized at normal values. During intervals of extreme irradiation variation of a cloudy day, DC voltage, active power, and reactive power have high fluctuations around rated values in case of without SC. With SC and RSA, DC voltage is stabilized rated and in most cases the active power fluctuates but less than without SC, while reactive power is almost zero. Variation temperature condition with constant irradiation, without SC, the DC voltage, active power, and reactive power high fluctuated around normal values. With SC connection, DC voltage, active power and reactive power are almost constant. Finally, the results showcase the ability of proposed optimized control technique of SC to overcome most fluctuations of system during abnormal conditions. Also, it improves the power quality and reliability of overall system because it makes system more flexible and stable. The calculation accuracy of control system parameters with SC and optimized technique has much better response if is compared with regular algorithms. RSA has a certain ability and advantage in solving the numerical problem for certain cases. Also, it improves the power quality and reliability of overall system because it makes system more flexible. A comparison study with and without the optimization technique is applied to the SC controller to examine the controller performance with PVS. Finally, Results of the studied PVS have shown the improved and effective performance under the variations of irradiation and temperature.

Acknowledgements

References

[1] A. Shaqour, H. Farzaneh, Y. Yoshida, and T. Hinokuma, "Power control and simulation of a building integrated stand-alone hybrid PV-wind-battery system in Kasuga City, Japan," Energy Reports, vol. 6, pp. 1528-1544, 2020.

[2] H. Ather, I. S. Zafar, and M. Hareem. "Review of the renewable energy status and prospects in Pakistan," International Journal of Smart Grid(ijSmartGrid), pp.167-73, 2021.

[3] Y. Cui, H. Yao, J. Zhang, K. Xian, T. Zhang, L. Hong, Y. Wang, Y. Xu, K. Ma, and C. An, "Single-junction organic photovoltaic cells with approaching 18% efficiency," Advanced Materials, vol. 32, p. 1908205, 2020.

[4] B. S. GOUD, C. R. Reddy, T. Rakesh, N. Rajesh, B. N. Reddy, and F. Aymen, "Grid Integration of Renewable Energy Sources using GA Technique for Improving Power Quality," International Journal of Renewable Energy Research (IJRER), vol. 11, pp. 1390-1402, 2021.

[5] M. Premkumar, C. Kumar, and R. Sowmya, "Mathematical Modelling of Solar Photovoltaic Cell/Panel/Array Based on the Physical Parameters from the Manufacturer's Datasheet," International Journal of Renewable Energy Development, vol. 9, 2020.

[6] A. I. Khalil, O. ISufian, H. N. Ghazi, S. Muhammad, and H. Nagmeldeen."Investigating the Effects of Solar Tracking Systems on Thermal Profile of Photovoltaic Modules". International Journal of Renewable Energy Research (IJRER), vol.11(4), p.1561-9, 2021

[7] R. Ahshan, R. Al-Abri, H. Al-Zakwani, N. Ambu-saidi, and E. Hossain, "Design and economic analysis of a solar photovoltaic system for a campus sports complex," International Journal of Renewable Energy Research (IJRER), vol. 10, pp. 67-78, 2020.

[8] K. Ece, and S. Gurkan. "Performance analysis of DC grid connected PV system under irradiation and temperature variations," in2019 8th International Conference on Renewable Energy Research and Applications (ICRERA), 2019,pp. 702-707.

[9] O. Lagdani, M. Trihi, and B. Bossoufi, "PV array connected to the grid with the implementation of MPPT algorithms (INC, P&O and FL method)," International Journal of Power Electronics and Drive Systems, vol. 10, p. 2084, 2019.

[10] J. Farzaneh, R. Keypour, and A. Karsaz, "A novel fast maximum power point tracking for a PV system using hybrid PSO-ANFIS algorithm under partial shading conditions," International Journal of Industrial Electronics, Control and Optimization, vol. 2, pp. 47-58, 2019.

[11] M. Mokhlis, M. Ferfra, and K. Chennoufi, "Experimental Test Bench of Photovoltaic Panel Under Partial Shading Effect Using the SLG-Backstepping technique," International Journal of Renewable Energy Research (IJRER), vol. 11, pp. 585-594, 2021.

[12] M. Mansoor, A. F. Mirza, and Q. Ling, "Harris hawk optimization-based MPPT control for PV Systems under Partial Shading Conditions," Journal of Cleaner Production, vol. 274, p. 122857, 2020.

[13] Y. Shan, J. Hu, and J. M. Guerrero, "A model predictive power control method for PV and energy storage systems with voltage support capability," IEEE Transactions on Smart Grid, vol. 11, pp. 1018-1029, 2019.

[14] M. C. Argyrou, F. Paterakis, C. Panagi, C. Makarounas, M. Darwish, and C. Marouchos, "Supercapacitor application for PV power smoothing," in 2018 53rd International Universities Power Engineering Conference (UPEC), 2018, pp. 1-5.

[15] S.-L. Wu, S.-S. Li, F.-C. Gu, P.-H. Chen, and H.-C. Chen, "Application of Super-Capacitor in Photovoltaic Power Generation System," in 2019 IEEE International Conference of Intelligent Applied Systems on Engineering (ICIASE), 2019, pp. 91-94.

[16] W. Jing, C. H. Lai, S. H. W. Wong, and M. L. D. Wong, "Battery-supercapacitor hybrid energy storage system in standalone DC microgrids: areview," IET Renewable Power Generation, vol. 11, pp. 461-469, 2016.

[17] M. Y. Worku, M. Abido, and R. Iravani, "Power fluctuation minimization in grid connected photovoltaic using supercapacitor energy storage system," Journal of Renewable and Sustainable Energy, vol. 8, p. 013501, 2016.

[18] K. Javed, H. Ashfaq, R. Singh, S. Hussain, and T. S. Ustun, "Design and performance analysis of a stand-alone PV system with hybrid energy storage for rural India," Electronics, vol. 8, p. 952, 2019.

[19] L. G. González, R. Chacon, B. Delgado, D. Benavides, and J. Espinoza, "Study of Energy Compensation Techniques in Photovoltaic Solar Systems with the Use of Supercapacitors in Low-Voltage Networks," Energies, vol. 13, p. 3755, 2020.

[20] Z. Fu, Z. Li, P. Si, and F. Tao, "A hierarchical energy management strategy for fuel cell/battery/supercapacitor hybrid electric vehicles," International journal of hydrogen energy, vol. 44, pp. 22146-22159, 2019.

[21] X. Ju, C. Xu, Y. Hu, X. Han, G. Wei, and X. Du, "A review on the development of photovoltaic/concentrated solar power (PV-CSP) hybrid systems," Solar Energy Materials and Solar Cells, vol. 161, pp. 305-327, 2017.

[22] A. Amir, H. S. Che, A. Amir, A. El Khateb, and N. Abd Rahim, "Transformerless high gain boost and buck-boost DC-DC converters based on extendable switched capacitor (SC) cell for stand-alone photovoltaic system," Solar Energy, vol. 171, pp. 212-222, 2018.

[23] A. Allagui, T. J. Freeborn, A. S. Elwakil, M. E. Fouda, B. J. Maundy, A. G. Radwan, Z. Said, and M. A. Abdelkareem, "Review of fractional-order electrical characterization of supercapacitors," Journal of Power Sources, vol. 400, pp. 457-467, 2018.

[24] O. Noureldeen, M. M. Youssef, and B. Hassanin, "Stability improvement of 200 MW Gabal El-Zayt wind farm connected to electrical grid using supercapacitor and static synchronous compensator during extreme gust," SN Applied Sciences, vol. 1, pp. 1-15, 2019.

[25] L. R. do Nascimento, T. de Souza Viana, R. A. Campos, and R. Rüther, "Extreme solar overirradiance events: Occurrence and impacts on utility-scale photovoltaic power plants in Brazil," Solar Energy, vol. 186, pp. 370-381, 2019.

[26] E. M. Deschamps and R. Rüther, "Optimization of inverter loading ratio for grid connected photovoltaic systems," Solar Energy, vol. 179, pp. 106-118, 2019.

[27] R. Nasrin, M. Hasanuzzaman, and N. A. Rahim, "Effect of high irradiation on photovoltaic power and energy," International Journal of Energy Research, vol. 42, pp. 1115-1131, 2018.

[28] M. Madhukumar, T. Suresh, and M. Jamil, "Investigation of Photovoltaic Grid System under Non-Uniform Irradiance Conditions," Electronics, vol. 9, p. 1512, 2020.

[29] O. Krishan and S. Suhag, "Grid-independent PV system hybridization with fuel cell-battery/supercapacitor: Optimum sizing and comparative techno-economic analysis," Sustainable Energy Technologies and Assessments, vol. 37, p. 100625, 2020

[30] A. Pareek, P. Singh, and P. N. Rao, "Analysis and Comparison of Charging Time between Battery and Supercapacitor for 300W Stand-Alone PV System," in 2018 International Conference on Current Trends towards Converging Technologies (ICCTCT), 2018, pp. 1-6.

[31] R. Z. Falama, S. Gamzat, H. Bakari, A. Dadjé, V. Dumbrava, S. Makloufi, and F. Tchangnwa, "Maximum Power Point Tracking of Photovoltaic Energy Systems Based on Multidirectional Search Optimization Algorithm," International Journal of Renewable Energy Research (IJRER), vol. 11, pp. 546-555, 2021.

[32] M. Chevalier, M. Gómez-Schiavon, A. H. Ng, and H. El-Samad, "Design and analysis of a proportional-integral-derivative controller with biological molecules," Cell systems, vol. 9, pp. 338-353. e10, 2019.

[33] S. Bassi, M. Mishra, and E. Omizegba, "Automatic tuning of proportional-integral-derivative (PID) controller using particle swarm optimization (PSO) algorithm," International Journal of Artificial Intelligence & Applications, vol. 2, p. 25, 2011.

[34] J. Kuo, K. Pan, N. Li, and H. Shen, "Wind Farm Yaw Optimization via Random Search Algorithm," Energies, vol. 13, p. 865, 2020.

[35] S. Abd Elazim and E. Ali, "Optimal power system stabilizers design via cuckoo search algorithm," International Journal of Electrical Power & Energy Systems, vol. 75, pp. 99-107, 2016.

[36] K. Sundareswaran, S. Peddapati, and S. Palani, "Application of random search method for maximum power point tracking in partially shaded photovoltaic systems," IET Renewable Power Generation, vol. 8, pp. 670-678, 2014.

[37] K. Sylevaster, and C. Erdal. "Photovoltaic System Efficiency Enhancement with Thermal Management: Phase Changing Materials (PCM) with High Conductivity Inserts," International Journal of Smart Grid(ijSmartGrid), pp.138-48, 2021.

[38] S. Lyden, H. Galligan, and M. E. Haque, "A Hybrid Simulated Annealing and Perturb and Observe Maximum Power Point Tracking Method," IEEE Systems Journal, 2020.

[39] D.S. Hyun D.Y. Lee, H.J. Noh and I.Choy, "An improved mppt converter using current compensation method for small scaled pvapplications," in Proc. APEC, 2003, pp. 540–545.

[40] S. A. Belfedhal, E. M. Berkouk, and Y. Messlem, "Analysis of grid connected hybrid renewable energy

system," Journal of Renewable and Sustainable Energy, vol. 11, p. 014702, 2019.

[41] A. Celia, B. Abdelhakim, C. Ilhami, G. Ouahib, and K. M. Akli. "Automatic and Self Adaptive P&O MPPT Based PID Controller and PSO Algorithm," in2021 10th International Conference on Renewable Energy Research and Application (ICRERA), 2021,pp. 385-390.

[42] K. Gunawardane, N. Bandara, K. Subasinghage, and N. Kularatna, "Extending the Input Voltage Range of Solar PV Inverters with Supercapacitor Energy Circulation. Electronics 2021, 10, 88," ed: s Note: MDPI stays neutral with regard to jurisdictional clai-ms in …, 2021.

[43] S. A. Mohamed, M. A. Tolba, A. A. Eisa, and A. M. El-Rifaie, "Comprehensive modeling and control of grid-connected hybrid energy sources using MPPT controller," Energies, vol. 14, p. 5142, 2021.

[44] A. Q. Al-Shetwi and M. Z. Sujod, "Modeling and control of grid-connected photovoltaic power plant with fault ride-through capability," Journal of Solar Energy Engineering, vol. 140, 2018.

[45] D. N. Luta and A. K. Raji, "Optimal sizing of hybrid fuel cell-supercapacitor storage system for off-grid renewable applications," Energy, vol. 166, pp. 530-540, 2019.

[46] A. AlKassem, M. AlAhmadi, and A. Draou."Modeling and Simulation Analysis of a Hybrid PV-Wind Renewable Energy Sources for a Micro-Grid Application," in2021 9th International Conference on Smart Grid (icSmartGrid), pp. 103-106, 2020.

[47] F. Nadeem, S. S. Hussain, P. K. Tiwari, A. K. Goswami, and T. S. Ustun, "Comparative review of energy storage systems, their roles, and impacts on future power systems," IEEE Access, vol. 7, pp. 4555-4585, 2018.

[48] W. Andari, G. Samir, H. Allagui, and A. Mami." Control strategy of fuel cell/supercapacitor hybrid propulsion system for anelectric vehicle". International Journal of Renewable Energy Research (IJRER),vol.10(1).p. 464-73.2020.

[49] J. S. Fadhil, and S. A. Mahmoud."Design and Simulation of a Boost-Microinverter for Optimized Photovoltaic System Performance," International Journal of Smart Grid (ijSmartGrid), pp. 94-102, 2021.

[50] Y.-P. Huang and P.-F. Tsai, "Improving the output power stability of a high concentration photovoltaic system with supercapacitors: a preliminary evaluation," Mathematical Problems in Engineering, vol. 2015, 2015.

[51] S. Najib and E. Erdem, "Current progress achieved in novel materials for supercapacitor electrodes: mini review," Nanoscale Advances, vol. 1, pp. 2817-2827, 2019.

[52] T.T. Guingan, D. Bonkoungou, E. Korsaga, E. Simonguy, Z. Koalaga, and F. Zougmore. "Modeling and Simulation of a Photovoltaic System Connected to the Electricity Grid with MALTAB/Simulink/Simpower Software," in 2020 8th International Conference on Smart Grid (icSmartGrid), 2020, pp.163-168.

[53] S. Peddapati, and K. K. Phanisri Kruthiventi. "A new random search algorithm: multiple solution vector approach." 2016 IEEE 6th International Conference on Advanced Computing (IACC). IEEE, 2016.

[54] W. Yunjing, H. Hongyun, and Q. Zhengwei, "PSO-PID based temperature control method for Bifilar Helix Calculable Resistor," in 2015 12th IEEE International.

[55] E. Victor, S. Tawat, S. Chatchai, U, Kasamsuk, and F. Olatubosun."Validation of Genetic Algorithm Optimized Hidden Markov Model for Short-term Photovoltaic Power Prediction." International Journal of Renewable Energy Research (IJRER), vol.11(2), pp.796-807, 2021.